19th Brazilian Congress of Thermal Sciences and Engineering
November 06th-10th, 2022, Bento Gonçalves - RS - Brazil

ENC-2022-0099
THERMAL EFFICIENCY AND SECOND LAW OF THERMODYNAMICS APPLIED IN A STRAIGHT MICROCHANNEL PRINTED CIRCUIT HEAT EXCHANGER

Élcio Nogueira
Faculdade de Tecnologia – FAT/UERJ, Rod. Pres. Dutra km 298, Resende, RJ, 27537-000, Brazil
elcionogueira@hotmail.com
Humberto Araújo Machado
Instituto de Aeronáutica e Espaço - IAE, Pç. Mal. Eduardo Gomes 50, São José dos Campos, SP, 12228-904, Brazil
Faculdade de Tecnologia – FAT/UERJ, Rod. Pres. Dutra km 298, Resende, RJ, 27537-000, Brazil
humbertoham@fab.mil.br

Abstract. *This work presents results from the application of a dimensionless theory that uses the concepts of thermal efficiency of heat exchangers and quantities associated with the second law of thermodynamics. The objective is to analyze the thermal and hydraulic performance in a Straight Microchannel Printed Circuit Heat Exchanger. Counter flow and parallel flow configurations were analyzed for water cooling using ethylene glycol based fluid and non-spherical platelet shaped Boehmite Alumina nanoparticles. Thermal efficiency, thermal effectiveness, thermal and viscous irreversibilities, thermodynamic Bejan number and outlet water temperatures are presented in graphical form. The data obtained allows concluding that the heat exchanger can work in a range of water and coolant flows below the design parameters. With the inclusion of nanoparticles, with a volume fraction equal to 5.0%, the flow rates of the refrigerant fluid may have a slight reduction. Through the analysis carried out, it is shown that the use of nanoparticles improves the operational cost-benefit of the heat exchanger with a significant reduction in the hot water outlet temperature.*

Keywords: *Printed circuit heat exchanger, Nanoparticles, Thermal efficiency, Second law of thermodynamic.*

1. INTRODUCTION

Printed circuit heat exchangers (PCHE) are devices fabricated by diffusion-bonding thin metal plates which were previously engraved with flow channels using chemical erosion techniques and present advantages concerned to mass production, reliability and economic efficiency. The use of nanofluids as heat exchangers work fluid may highly increase the thermal efficiency of such equipment. In this work, a PCHE performance is simulated when a nanofluid is employed.

Seo et al. (2015) performed performance tests on a micro-channel printed circuit heat exchanger (PCHE) in a single-phase regime. In counterflow and parallel flow configurations, Reynolds numbers ranged from 100 to 850. They developed empirical correlations for heat transfer coefficient and pressure drop as functions of the Reynolds number.

Rosa et al. (2009) state inconsistencies between results published in recent decades for single-phase microscale heat transfer and that there is still no consensual model. They review experimental and numerical models available in the open literature, clarify that scale effects, often insignificant in macro channels, can significantly influence the results and must be carefully considered and they call attention to measurement uncertainties due to their reduced characteristic dimensions.

Alon et al. (2021) present a multilayer printed circuit heat exchanger prototype with 17 transparent plates photochemically bonded by diffusion. They measure pressure losses and heat transfer in zigzag flow geometry and orientation of glued shims. Results are available in a dimensionless form to facilitate comparisons with thermo-hydraulic correlations. Two fluids with drastically different properties provide a unique method of exploring the effect of the working fluid on PCHE performance

Baik et al. (2015) developed a PCB exchanger design and analysis code to predict thermohydraulic performance. The range of Reynolds numbers considered corresponds to 2000-58000. A prototype was manufactured to test the

accuracy of the developed code. The experimental results demonstrated acceptable thermal performance and small pressure losses. The experimental results showed effectiveness above 90% in a small core of 200 mm.

Chai and Tassou (2020) review and establish a comprehensive understanding of printed circuit heat exchangers (PCHEs). The study covered existing heat exchangers on the market and projects under development. They conclude that more work is needed to increase the range of applications for printed circuit heat exchangers. Zhao et al. (2019) study a promising plate-type heat exchanger, the printed circuit (PCHE) of high compactness, suitable for high-pressure conditions. They investigate the thermohydraulic performance numerically of the heat exchanger using the SST k-ω turbulence model and evaluate heat transfer and pressure loss and loss using Nusselt and Euler numbers. To define better-operating conditions, they propose the Nu/Eu ratio for a comprehensive evaluation of the heat exchanger, considering thermal and hydrodynamic aspects and conclude that thermal performance is better with a higher mass flow and lower operating pressures. Bhosale and Acharya (2020) state that microchannels can be explored as turbine blades, rocket engines, hybrid vehicles, refrigeration cooling, thermal control in microgravity, and microgravity heat sinks channels may be the solution to 21st-century cooling problems.

Tanga et al. (2022) numerically analyze the effect of axial heat conduction on thermal performance in a zigzag channel printed circuit heat exchanger (PCHE). The analysis includes Reynolds number, operating pressure, cold side inlet temperatures, and wall thermal conductivity.

Timofeeva et al. (2009) experimentally investigate various alumina nanoparticles' thermal conductivity and viscosity in a fluid consisting of an equal amount of water and ethylene glycol. They develop a theoretical model for the analysis of experimental data. They claim that the presence of small fractions of nanoparticles significantly increases the viscosity of the suspension due to structural constraints

Monfared et al. (2019) studied nanoparticle shape's effects on entropy generation in Boehmite alumina nanofluid flow in a double tube heat exchanger. Non-spherical nanoparticles are of the brick, sheet, platelet, and cylindrical type, suspended in a water and ethylene glycol mixture. Water flows from the annular side of the heat exchanger. The influence of the Reynolds number on the thermal and total entropy generation rates through the Bejan number was investigated numerically.

In this work a dimensionless theory that uses the concepts of thermal efficiency of heat exchangers and quantities associated with the second law of thermodynamics is applied to estimate the influence of the refrigerant flow rate and the effect of the inclusion of non-spherical Alumina Boehmite nanoparticles on the thermohydraulic performance of a microchannel PCHE. The volume fraction of nanoparticles in the form of platelets corresponds to 5.0% of the volume of the refrigerant fluid, composed of 50% ethylene glycol. The fluid to be cooled is water at an initial temperature of 98°C. A dimensionless analysis applies the definition of thermal efficiency in heat exchangers and the second law of thermodynamics for counter-flow and parallel-flow configurations.

2. METHODOLOGY

Figures (1.a,b) were extracted from theoretical and experimental work prepared by Seo et al. (2015). The author performed thermal and dynamic performance tests for a PCHE. The tests were carried out for configuration in counterflow, for Reynolds numbers in the range of 100–850, with inlet temperatures equal to 50º and 20º. Developed empirical correlations for the heat transfer coefficient as a function of the Reynolds number for both fluids, Equations (12) and (13). Table 1 presents the properties of hot and cold fluids and Boehmite Alumina Platelet Nanoparticles. Table 2 characterizes the viscosity and thermal conductivity of the nanoparticle in the form of a platelet, Equations (6) and (8).

Table 1. Fluid and nanoparticle properties, hot (Water), cold (Ethylene Glycol), platelets of Boehmite Alumina (Timofeeva et al., 2009; Monfared et al., 2019).

	ρ kg/m^3	**k W/ (m K)**	**Cp J/(kg K)**	**μ kg/(m s)**	**N m/s^2**	**A m/s^2**	**Pr**
Quente	994	0.623	4178	$0.72\ 10^{-3}$	$7.24\ 10^{-7}$	$1.5\ 10^{-7}$	4.83
Frio	1067.5	0.3799	3300	$3.39\ 10^{-3}$	$2.4045\ 10^{-5}$	$1.08\ 10^{-7}$	0.02
B Alumina	3050	30	618.3	-	-		-

Table 2. Coefficients that characterize the non-spherical shape of nanoparticles in dynamic viscosity and thermal conductivity (Monfared et al., 2019).

Type	**C_k**	**A_1**	**A_2**
Platelet	2.61	37.1	612.6

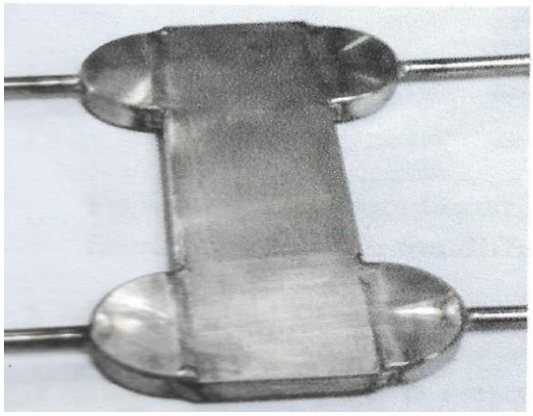

(a) PCHE external view

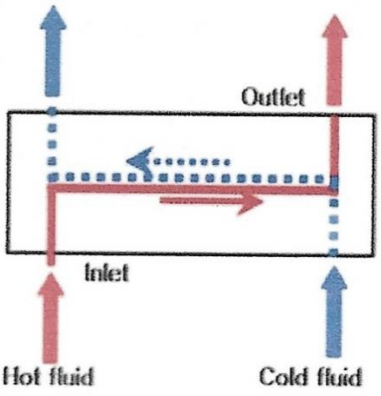

(b) Schematic representation of counter current flow in PCHE

Figure 1. PCHE studied in the work of Seo et al. (2015).

2.1 Procedure for thermal analysis

The parameters considered for simulation were: φ = 0.05, Th_i = 98.0 °C, Tc_i = 98.0 °C, Re_h = 200 and Re_c = Re*Re_h, where φ is the volume fraction of the nanoparticles. Th_i and Tc_i are the inlet temperatures for hot and cold fluids, respectively. Re_h is the Reynolds number associated with the hot fluid and Re_c is the ratio of the Reynolds number of the cold fluid to the Reynolds number of the hot fluid.

$$Dh_c = \frac{4A_{cc}L_f}{As_c} \tag{1}$$

where Dh_c is the hydraulic diameter, A_{cc}=42.2 x 10^{-6} m^2, Lf_c = 137 x 10^{-3} m is the channel length, As_c =34.716 x 10^{-3} m^2 is the heat transfer area for the cold fluid.

$$Dh_h = Dh_c \tag{2}$$

$$Lf_h = \frac{Dh_h As_h}{4Ac_c} \tag{3}$$

where Lf_h is the channel length, As_h =26.037 x 10^{-3} m^2 is the heat transfer area for the hot fluid. The properties of the nanofluid are obtained by:

$$\rho_{nano} = \rho_{Particle}\varphi + (1-\varphi)\rho_c \tag{4}$$

$$\mu_{nano} = \frac{\mu_c}{(1-\varphi)^{2.5}} \tag{5}$$

$$Cp_{nano} = \frac{Cp_{Particle}\,\rho_{Particle}\,\phi + (1-\phi)\,Cp_C\,\rho_C}{\rho_{nano}} \tag{6}$$

$$k_{nano} = \frac{[k_{Particle} + 2\,k_C + 2\,(k_{Particle} - k_C)\,(1-0.1)^3\,\phi]}{[k_{Particle} + 2\,k_C + 2\,(k_{Particle} - k_C)\,(1-0.1)^2\,\phi]}\,K_c \tag{7}$$

$$\nu_{nano} = \frac{\mu_{nano}}{\rho_{nano}} \tag{8}$$

$$\alpha_{nano} = \frac{k_{nano}}{\rho_{nano}\,Cp_{nano}}\,Cp_{nano} = \frac{Cp_{Particle}\,\rho_{Particle}\,\phi + (1-\phi)\,Cp_C\,\rho_C}{\rho_{nano}} \tag{9}$$

$$Pr_{nano} = \frac{\mu_{nano}}{\alpha_{nano}} \tag{10}$$

$$\mu_W = \frac{\mu_{nnao} + \mu_h}{2} \tag{11}$$

where μ_W is the assumed value for the fluid's viscosity at the channel wall.

$$h_{nano} = 0.1706\ 6^{0.44}\ Re_{nano}{}^{0.324}\ Pr_{nano}{}^{\frac{1}{3}}\ \left(\frac{\mu_{nano}}{\mu_W}\right)^{0.14}\left(\frac{k_{nano}}{Dh_C}\right)\mu_W = \frac{\mu_{nnao}+\mu_h}{2} \tag{12}$$

$$h_h = 0.1729\ 5^{0.44}\ Re_h{}^{0.324}\ Pr_h{}^{1/3}\ \left(\frac{\mu_h}{\mu_W}\right)^{0.14}\left(\frac{k_h}{Dh_h}\right) \tag{13}$$

The heat transfer coefficients of both fluids, cold (h_{nano}) and hot (h_h), were obtained by regression fit (Steinke and Kandlikar, 2005).

$$A_{Med} = \frac{As_h + As_C}{2} \tag{14}$$

The overall heat transfer coefficient is obtained by:

$$UoA = \frac{1}{\frac{1}{h_h\ As_h} + \frac{1}{h_{nano}\ As_C} + \frac{L}{k_{Metal}\ A_{Med}}} \tag{15}$$

k_{Metal} = 16.2 W/mK is the thermal conductivity of the heat transfer plate and L = 0.4 x 10^{-3} m is the thickness between the cold and hot channels.

$$\dot{m}_h = \frac{Re_h\ \mu_h\ Ac_h}{Dh_h} \tag{16}$$

$$\dot{m}_{nano} = \frac{Re_{nano}\ \mu_{nano}\ Ac_C}{Dh_C} \tag{17}$$

$$\dot{m}^* = \frac{\dot{m}_{nano}}{\dot{m}_h} \tag{18}$$

where $\dot{m}_h$ and $\dot{m}_{nano}$ are the mass flow rates of the hot and cold fluid, respectively.

$$C_h = \dot{m}_h\ Cp_h \tag{19}$$

$$C_{nano} = \dot{m}_{nano}\ Cp_{nano} \tag{20}$$

C_h and C_{nano} are the heat capacities of the hot and cold fluids, respectively.

$$C^* = \frac{C_{min}}{C_{max}} \tag{21}$$

where C_{min} is the minimum value between C_h and C_{nano}.

$$NTU = \frac{UoA}{C_{min}} \tag{22}$$

where *NTU* is the number of thermal units associated with the heat exchanger.

$$Fa = \frac{NTU\ (1-C^*)}{2}\ for\ counter\ flow \tag{23.a}$$

$$Fa = \frac{NTU\ (1+C^*)}{2}\ for\ parallel\ flow \tag{23.b}$$

where *Fa* is the fin analogy for heat exchanger (Fakheri, 2007; Nogueira, 2020).

$$\eta_T = \frac{tanh(Fa)}{Fa} \tag{24}$$

η_T is the thermal efficiency.

$$\varepsilon_T = \frac{1}{\frac{1}{\eta_T\ NTU} + \frac{1+C^*}{2}} \tag{25}$$

where ε_T is the thermal effectiveness.

$$\dot{Q}_{Max} = (Th_i - Tc_i)\, C_{min} \tag{26}$$

where $\dot{Q}_{Max}$ is the maximum heat transfer rate for the situation under analysis.

$$\dot{Q} = \frac{(Th_i - Tc_i)\, C_{min}}{\frac{1}{\eta_T\, NTU} + \frac{1+C^*}{2}} \tag{27}$$

where $\dot{Q}$ is the actual rate of heat transfer. The outlet temperatures for both fluids, Th_0 and Tc_0, are obtained by:

$$Th_O = Th_i - \frac{\dot{Q}}{\dot{m}\, Cp_h} \tag{28}$$

$$Tc_O = Tc_i - \frac{\dot{Q}}{\dot{m}\, Cp_{nano}} \tag{29}$$

$$\sigma_T = \left(\frac{C_h}{C_{min}}\right) ln\left(\frac{Th_o}{Tc_i}\right) + \left(\frac{C_{nano}}{C_{min}}\right) ln\left(\frac{Tc_o}{Tc_i}\right) \tag{30}$$

where σ_T is the thermal irreversibility of the heat exchanger.

2.2 Procedure for hydrodynamic analysis

Naming D_P as the diameter of the entrance port, this parameter is fixed as: $D_p = 0.\ X\ 10^{-3}\ m$.

$$Gc = \frac{\dot{m}_c}{Ac_c} \tag{31}$$

$$Gh = \frac{\dot{m}_h}{Ac_h} \tag{32}$$

$$Gp_c = \frac{4\dot{m}_c}{\pi {D_P}^2} \tag{33}$$

$$Gp_h = \frac{4\dot{m}_h}{\pi {D_P}^2} \tag{34}$$

where Gc and Gh are the mass fluxes of the cold and hot fluids, respectively. Gp_c and Gp_h are the mass flows through the portals.

$$fc_c = \frac{0.316}{Re_{nano}^{0.25}} \tag{35}$$

$$fc_h = \frac{0.316}{Re_h^{0.25}} \tag{36}$$

$$fc_{Exp} = \frac{1.3383}{Re_{nano}^{0.5003}} \tag{37}$$

$$fh_{Exp} = \frac{1.3383}{Re_h^{0.5003}} \tag{37}$$

where fc_c and fc_h are the theoretical friction factors associated with hot and cold fluids; fc_{Exp} and fh_{Exp} are the experimental coefficients of friction (Steinke and Kandlikar, 2005).

$$\Delta P_c = \frac{4 fc_c L f_c Gc^2}{2 Dh_c \rho_{nano}} \tag{38}$$

$$\Delta P_h = \frac{4 fc_h L f_h Gh^2}{2 Dh_h \rho_h} \tag{39}$$

$$\Delta P_{Pc} = \frac{1.5 {Gp_c}^2}{2\rho_{nano}} \tag{40}$$

$$\Delta P_{Ph} = \frac{1.5 G {p_h}^2}{2\rho_h} \tag{41}$$

ΔP_c and ΔP_h are the pressure drops along the channels; ΔP_{pc} and ΔP_{ph} are the pressure drops in the portals. It is assumed that $P_{2h} = P_{2c} = P_{Atm}$
$P_{1c} = \Delta P_c + \Delta P_{pc} + P_{2c}$.

$$P_{1c} = \Delta P_c + \Delta P_{pc} + P_{2c} \tag{42}$$

$$P_{1h} = \Delta P_h + \Delta P_{ph} + P_{2h} \tag{43}$$

$$\sigma_f = -\left(\frac{C_h}{C_{min}}\right) R\ ln\left(\frac{P_{2h}}{P_{1h}}\right) - \left(\frac{C_{nano}}{C_{min}}\right) R\ ln\left(\frac{P_{2c}}{P_{1c}}\right) \tag{44}$$

$$R = \frac{Th_i - Th_o}{Tc_o - Tc_i} \tag{45}$$

Then:

$$S_{genf} = \sigma_f C_{min} \tag{46}$$

Where σ_f and S_{genf} are the viscous irreversibility and the entropy generation rate (Bejan, 1987). Finally:

$$Be = \frac{S_{gent}}{S_{gent} - S_{genf}} \tag{47}$$

Where *Be* is the thermodynamic Bejan number (Bejan, 1987; Fakheri, 2007).

3. RESULTS AND DISCUSSION

Figure 2 shows the relationships between the mass flows of fluids within the working range between them. The hot fluid flow corresponds to a fixed Reynolds number equal to 200, and the coolant flow corresponds to a variation for the Reynolds number between 50 and 1000. When you have ethylene glycol flowing, with zero nanofluid mass fraction, the change in mass of the cold fluid is not significantly more significant when compared to the flow rate of the hot fluid. For $Re_c=1000$, that is, $Re^*=5$, the ratio between the masses of the cold fluid by the hot fluid is approximately equal to 20. However, when fractions of nanoparticles are included, the mass flow increases significantly with the increase in the number of nanoparticles. Reynolds is associated with soda. When $Re_{nano}=200$, i.e., $Re^*=1$, the nanofluid mass flow rate approximately corresponds to the ethylene glycol mass flow rate for Re*=5. This increase in mass flow significantly affects all parameters that will be analyzed in the context of this work.

Figure 3 shows the variation in the number of thermal units associated with the heat exchanger for the two situations under analysis: a flow of 50% pure ethylene glycol and a flow of 50% ethylene glycol plus 0.05 volume fraction Alumina Boehmite nanoparticles. For low flow rates of the refrigerant fluid, a significant increase in the number of thermal units of the nanofluid can be observed compared to the number of thermal units of the 50% pure ethylene glycol. However, the initial difference becomes less pronounced for high flow rates of the refrigerant fluid, tending to a limit value when $Re^* = 5$.

The same occurs with the relationship between the thermal capacities of both fluids, Figure 4, with a significant difference for low flows and a slight difference for higher flows. These two parameters, NTU and C*, are primarily responsible for determining the thermal efficiency of the heat exchanger, as defined in this work. The thermal efficiency of the heat exchanger is shown in Figure 5. In this context, the thermal efficiency represents the potential for heat exchange between the fluids. When the efficiency approaches 1, there is the maximum potential for heat exchange. After that, the heat exchange between the fluids tends to a minimum value, and this potential tends to zero. For example, there is a high heat exchange potential for 50% ethylene glycol at low refrigerant flow rates and an approximate 10% drop for nanofluid at a volume fraction equal to 0.05. It can be anticipated, in this case, that the potential presented by ethylene glycol was better used when introducing nanoparticles.

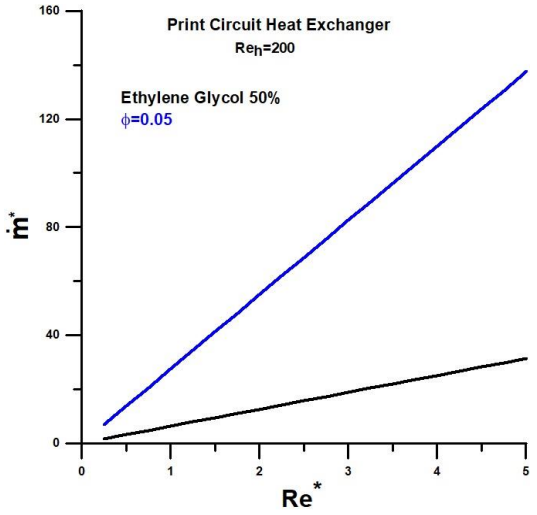

Figure 2. Ratio of mass flow rates of the cold fluid to the hot fluid.

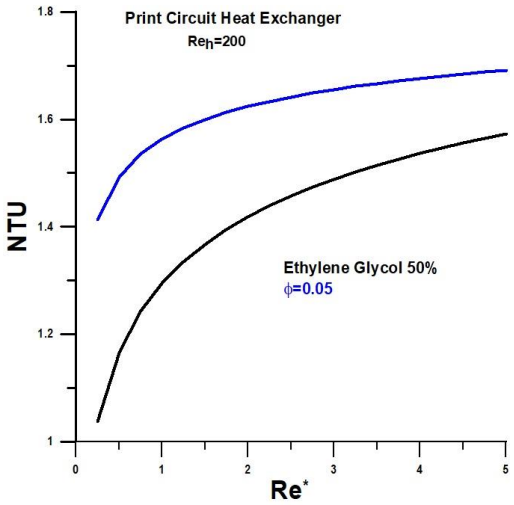

Figure 3. Number of thermal units (NTU) versus the ratio of Reynolds numbers.

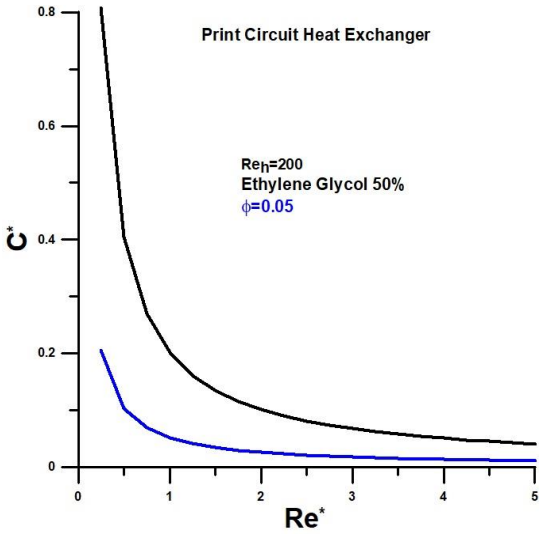

Figure 4. Ratio of heat capacities versus the ratio of Reynolds numbers.

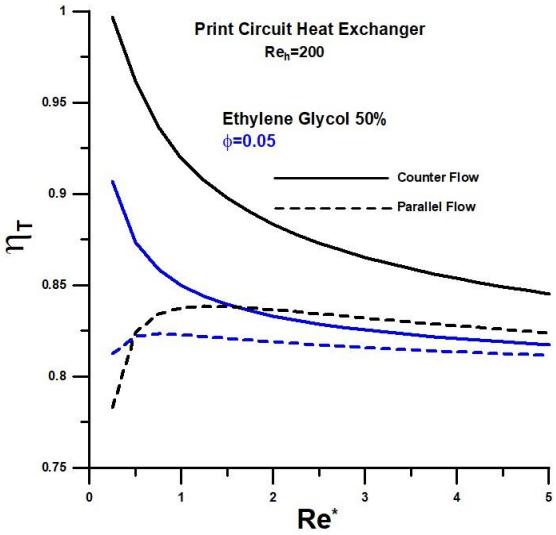

Figure 5. Thermal efficiency versus the ratio of Reynolds numbers.

When comparing the relationship between the heat transfer rates, represented by the thermal effectiveness, Figure 6 shows that the heat transfer rate associated with the nanofluid is higher than that of ethylene glycol by 50%. In this case, it is observed again that the greatest difference occurs for lower refrigerant flows. For the lowest flow rate of the refrigerant, there is an approximate increase of 27% in the heat transfer rate when adding the nanofluid, and this value drops to approximately 6% for high flow rates. Regarding the two heat exchanger configurations under analysis, counterflow and parallel flow, it is evident that there is greater heat exchange for the counterflow type exchanger.

The thermal effectiveness of the heat exchanger is very similar to what is observed for the thermal irreversibility, Figure 7, making it evident that these are equivalent quantities when comparing the thermal performance of the heat exchanger. Regarding the last two analyzed quantities, thermal effectiveness, and thermal irreversibility, it should be noted that none of them makes it possible to determine the absolute value of the heat transfer rate that occurs during the exchange process between fluids. Instead, they only indicate how close or far away the heat transfer rate is concerning the maximum possible heat transfer rate.

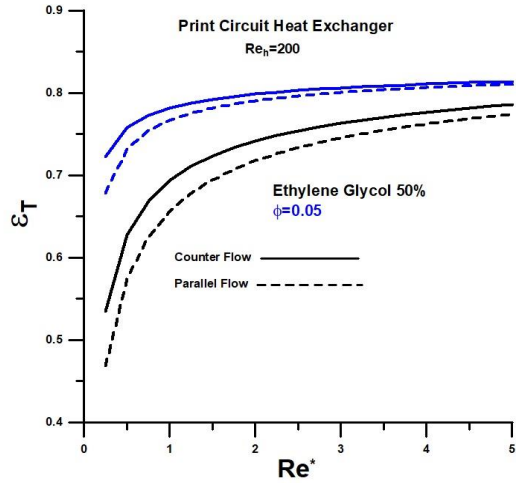

Figure 6. Thermal effectiveness versus the ratio of Reynolds numbers.

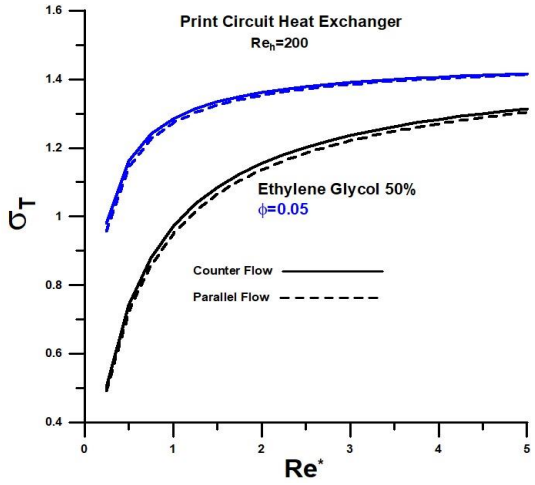

Figure 7. Thermal irreversibility versus the ratio of Reynolds numbers.

For a systemic analysis of the heat exchanger, considering quantities related to heat exchange and viscous dissipation, it becomes relevant to determine quantities associated with hydrodynamic aspects. The most pertinent parameter related to the flow is the friction factor. Just as the Nusselt number modulates the heat transfer, it effectively determines the pressure drop in the flow. Figure 8 presents theoretical and empirical results for the friction factor for comparison purposes. The empirical correlation was obtained through experimental results determined by Steinke and Kandlikar (2005) and the theoretical expression presented by Bhosale and Acharya (2020). In this work, we chose to use empirical correlation to determine the magnitudes dependent on the friction factor since the results obtained experimentally are within the Reynolds numbers of the designed device.

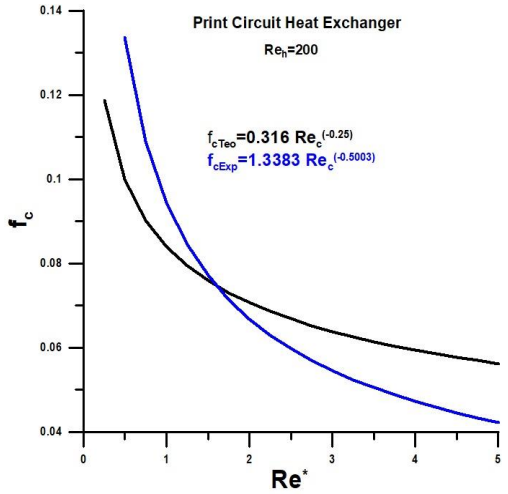

Figure 8. Friction factor versus the ratio of Reynolds numbers.

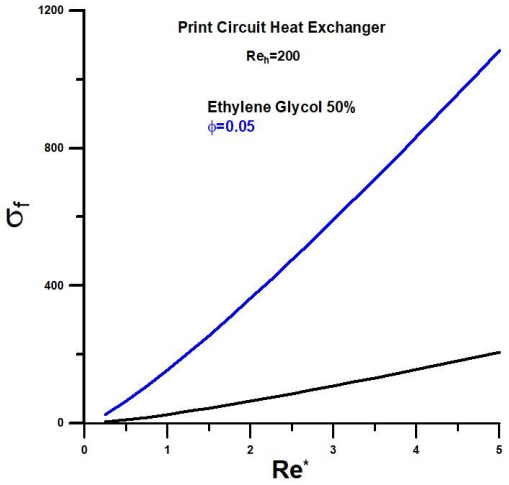

Figure 9. Viscous irreversibility versus the ratio of Reynolds numbers.

The viscous irreversibility is represented in Figure 9, as a function of the refrigerant fluid flow, with and without the inclusion of nanoparticles fraction. As already observed, when fractions of nanoparticles are included in the flow, the mass flow increases, significantly affecting the viscous irreversibility. In this case, the addition is exceptionally high for higher flows, preliminarily indicating the impossibility of working at the upper limit of flows for the refrigerant. At lower flow rates, however, the viscous dissipation added by the nanoparticles is of the same order of magnitude as the viscous dissipation caused by 50% pure ethylene glycol. Therefore, it is expected that nanoparticles can be used for lower refrigerant flow rates.

The ratio between thermal irreversibility and total irreversibility is represented in Figure 10 through the Bejan thermodynamic number for a counterflow heat exchanger. At lower flow rates for the refrigerant, the thermal irreversibility is of the order of magnitude of the total irreversibility, which indicates a non-prevalence of viscous irreversibility. However, with the increase in the flow rate for the refrigerant, the Bejan number presents shallow values.

It tends to a minimum value at medium and high flows, with significant relevance for the nanofluid concerning 50% pure ethylene glycol.

The data show that the heat exchanger should not work in the upper flow rate range for the refrigerant for a favorable cost-benefit ratio. However, the reasonable flow limit for 50% pure ethylene glycol is higher than the practical flow limit for the nanofluid. Preliminarily, based on the Bejan number, the threshold value for the Reynolds number in ethylene glycol is approximately equal to Re*=3, and for the nanofluid, Re*=1 is a probable indicator.

The absolute values for the hot fluid outlet temperatures, when Reh=200, are represented in Figure 11. The results obtained corroborate the previous conclusions and allow a decision of the flow ranges where a cost-benefit ratio is advantageous. For low flows, the temperature drop is significant. Still, from a given value, the decrease in temperature is negligible and does not justify the effort and energy consumption in the form of viscous dissipation. Therefore, we indicate again that the justifiable threshold flow for nanofluid corresponds to approximately Re*=1, and for 50% pure ethylene glycol, Re*=3 is a reasonable threshold value.

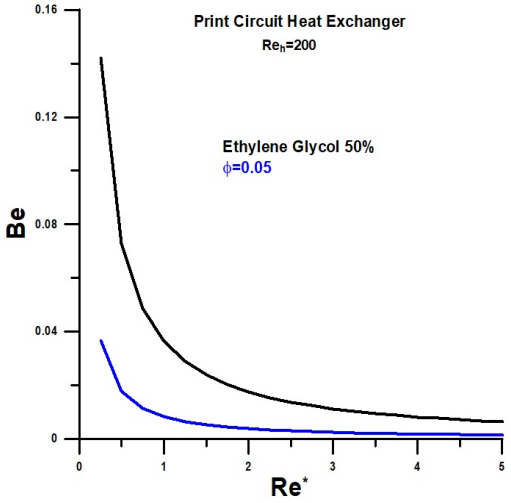

Figure 10. Bejan number versus the ratio of Reynolds numbers.

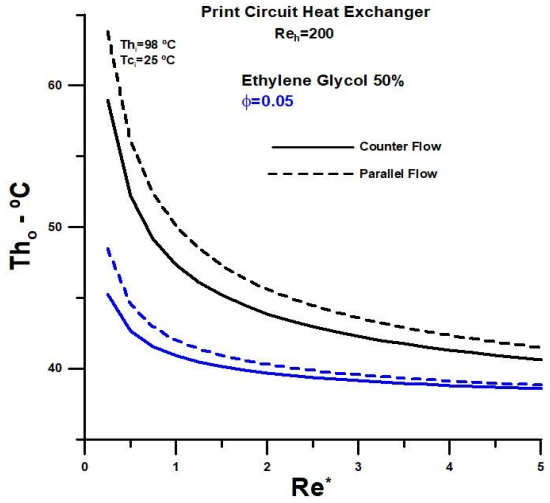

Figure 11. Hot outlet temperature versus the ratio of Reynolds numbers.

In summary, it is about the application of an analytical method, with purely algebraic procedures. Simple, elegant and physically consistent, with physical, geometric, and empirical quantities taken from theoretical and experimental work by Seo J. et al. (2015). The most important empirical quantities used in this work are the heat transfer coefficients (Equations 12 and 13) experimentally determined for the flow rate used in the device under analysis.

4. CONCLUSION

The work presents results from applying a dimensionless theory that uses the concepts of thermal efficiency in heat exchangers and quantities associated with the second law of thermodynamics. Thermohydraulic performance analysis was performed on a straight microchannel printed circuit heat exchanger. Counter-flow and parallel-flow configurations were analyzed for water cooling using 50% ethylene glycol base fluid and platelet-shaped non-spherical Boehmite Alumina nanoparticles. The heat exchanger was designed to work in a range of Reynolds numbers between 200 and 850. However, high values for the Reynolds number increase viscous dissipation and lead to a degradation of the thermal potential, which is amplified with the inclusion of nanoparticles.

It is concluded that the heat exchanger under analysis must operate at low flow rates for the refrigerant fluid, where the potential for heat exchange remains high and reasonably above a minimum threshold. For lower refrigerant flows, viscous irreversibilities are relatively low concerning thermal irreversibilities, allowing a viable cost-benefit for the heat exchanger, even with nanoparticles at a volume fraction equal to 5.0%. It is proven that what should act to improve the thermal performance of the heat exchanger works in the sense of increasing viscous dissipations. It is shown that the dimensionless analysis of heat exchangers, in the form presented, is a valuable tool for thermo-hydraulic optimization of heat exchangers.

5. REFERENCES

Baik, S., Kim, S. G., Son1, S., Kim, H. T. and Lee, J. I., 2015. "Printed Circuit Heat Exchanger Design, Analysis and Experiment", *NURETH-16, Chicago, IL*, August 30-September 4.

Bejan, A., 1987. "The Thermodynamic Design of Heat And Mass Transfer Processes and Devices", *Heat and Fluid Flow*, Vol. 8, No. 4, pp. 258-276.

Bhosale, S .S. and Acharya, A. R., 2020. "Review On Applications of Micro-Channel Heat Exchanger", *International Research Journal of Engineering and Technology (IRJET)*, Volume: 07 Issue: 03.

Chai, L. and Tassou, S. A., 2020. "A Review of Printed Circuit Heat Exchangers for Helium and Supercritical CO2 Brayton Cycles", *Thermal Science and Engineering Progress*, 18 (2020) 100543.

Fakheri, A., 2007, "Heat Exchanger Efficiency", *Transactions of the ASME*, Vol. 129, pp. 1268- 1276.

Katz, A., Aakre, S. R., Anderson, M. H. and Ranjan, D., 2021, *Experimental Investigation of Pressure Drop and Heat Transfer in High-Temperature Supercritical CO2 and Helium in a Printed-Circuit Heat Exchanger*, Published by Elsevier (This manuscript is made available under the Elsevier user license).

Monfared, M., Shahsavar, A., Bahrebar, M. R., 2019, "Second Law Analysis of Turbulent Convection Flow of Boehmite Alumina Nanofluid Inside a Double-Pipe Heat Exchanger Considering Various Shapes For Nanoparticle", *Journal of Thermal Analysis and Calorimetry* (2019) 135:1521–1532.

Nogueira, E., 2020, "Thermal Performance in Heat Exchangers by the Irreversibility, Effectiveness and Efficiency Concepts Using Nanofluids", *Journal of Engineering Sciences*, 7: F1-F7.

Rosa, P., Karayiannis. T.G., Collins and M.W., 2009, "Single-Phase Heat Transfer in Microchannels: the Importance of Scaling Effects", *Applied Thermal Engineering* . DOI: 10.1016/j.applthermaleng.2009.05.015

Seo, J., Kim, Y., Kim, D., Choi, Y., and Lee, K., 2015. "Heat Transfer and Pressure Drop Characteristics in Straight Microchannel of Printed Circuit Heat Exchangers", *Entropy*, 17, 3438-3457. DOI: 10.3390/e17053438

Steinke, M. E. and Kandlikar, S. G., 2005, "Single-Phase Liquid Heat Transfer in Microchannels", in *Proceedings of ICMM2005 3rd International Conference on Microchannels and Mini Channel*, June 13-15, 2005, Toronto, Ontario, Canada.

Tanga, L., Yanga, B., Pan, J. and Sunden, B., 2022, "Thermal Performance Analysis in a Zigzag Channel Printed Circuit Heat Exchanger under Different Conditions", *Heat Transfer Engineering*, 43:7, 567-583.

Timofeeva, E. V., Routbort, J. L. and Singh, D., 2009, "Particle Shape Effects on Thermophysical Properties of Alumina Nanofluids", *Journal of Applied Physics*, 106, 014304.

Zhao, Z., Zhou, Y., Ma, X., Chen, X., Li, S. and Yang, S., 2019, "Numerical Study on Thermal-Hydraulic Performance of Supercritical LNG in Zigzag-Type Channel PCHEs", *Energies*, 12, 548.

6. RESPONSIBILITY NOTICE

The authors are the only responsible for the printed material included in this paper.